



## Article

# Mapping Agronomic and Quality Traits in Elite Durum Wheat Lines under Differing Water Regimes

Rosa Mérida-García <sup>1</sup>, Alison R. Bentley <sup>2</sup>, Sergio Gálvez <sup>3</sup>, Gabriel Dorado <sup>4</sup>,  
Ignacio Solís <sup>5</sup>, Karim Ammar <sup>6</sup> and Pilar Hernandez <sup>1,\*</sup>

<sup>1</sup> Institute for Sustainable Agriculture (IAS-CSIC), Consejo Superior de Investigaciones Científicas (CSIC), Alameda del Obispo s/n, 14004 Córdoba, Spain; rmerida@ias.csic.es

<sup>2</sup> The John Bingham Laboratory, NIAB, Huntingdon Road, Cambridge CB3 0LE, UK; alison.bentley@niab.com

<sup>3</sup> Departamento de Lenguajes y Ciencias de la Computación, Campus de Teatinos s/n, Universidad de Málaga, Andalucía Tech, ETSI Informática, 29071 Málaga, Spain; galvez@uma.es

<sup>4</sup> Departamento de Bioquímica y Biología Molecular, Campus Rabanales C6-1-E17, Campus de Excelencia Internacional Agroalimentario (ceiA3), Universidad de Córdoba, 14071 Córdoba, Spain; bb1dopeg@uco.es

<sup>5</sup> ETSIA (University of Seville), Ctra de Utrera km1, 41013 Seville, Spain; isolis@agrovetal.es

<sup>6</sup> International Maize and Wheat Improvement Center (CIMMYT), C.A.P. Plaza Galerías, Col. Verónica Anzures, Ciudad de Mexico 11305, Mexico; k.ammar@cgiar.org

\* Correspondence: phernandez@ias.csic.es

Received: 17 December 2019; Accepted: 14 January 2020; Published: 19 January 2020



**Abstract:** Final grain production and quality in durum wheat are affected by biotic and abiotic stresses. The association mapping (AM) approach is useful for dissecting the genetic control of quantitative traits, with the aim of increasing final wheat production under stress conditions. In this study, we used AM analyses to detect quantitative trait loci (QTL) underlying agronomic and quality traits in a collection of 294 elite durum wheat lines from CIMMYT (International Maize and Wheat Improvement Center), grown under different water regimes over four growing seasons. Thirty-seven significant marker-trait associations (MTAs) were detected for sedimentation volume (SV) and thousand kernel weight (TKW), located on chromosomes 1B and 2A, respectively. The QTL loci found were then confirmed with several AM analyses, which revealed 12 sedimentation index (SDS) MTAs and two additional loci for SV (4A) and yellow rust (1B). A candidate gene analysis of the identified genomic regions detected a cluster of 25 genes encoding blue copper proteins in chromosome 1B, with homoeologs in the two durum wheat subgenomes, and an ubiquinone biosynthesis O-methyltransferase gene. On chromosome 2A, several genes related to photosynthetic processes and metabolic pathways were found in proximity to the markers associated with TKW. These results are of potential use for subsequent application in marker-assisted durum wheat-breeding programs.

**Keywords:** durum wheat; genome wide association study; GWAS water use; agronomic traits; MTAs; candidate genes; TKW; sedimentation volume; SDS; YR

## 1. Introduction

Wheat is one of the most widely grown crops worldwide (FAO, 2015), and is essential for the human diet [1]. Its importance and worldwide dominance are due, in part, to its agronomic adaptability. Durum wheat (*Triticum durum*) is a tetraploid wheat species (AABB genomes) mainly grown in the Mediterranean basin, in the Northern Plains (between the USA and Canada), in the arid areas of South Western USA and in Northern Mexico [2]. Durum wheat is well-adapted to a broad range of climatic conditions (including dry environments) and marginal soils, and has low water requirements [3,4]. Climatic conditions, as temperature and water availability, together with biotic stresses, can strongly affect durum wheat development and production [3–6]. Crop adaptation

is a central objective for breeding progress, driving improvement in final production, quantity and quality [7,8]. For over two decades, CIMMYT (International Maize and Wheat Improvement Center) has had an intensive breeding and improvement programme focused on the acceleration of durum productivity in developing countries.

Grain quality is an important breeding aim determining product end-use linked to financial returns. It is influenced by both genetic and environmental conditions [9], and biotic and abiotic stresses during growth and at key development stages [10]. Temperature, water availability and soil properties, especially nitrogen content, influence the final quality and protein content of wheat and its end-products [11–13].

There is a growing need to increase wheat yield without losing grain quality [14,15]. Key end-use grain quality traits include grain protein content (GPC), gluten strength, kernel size and vitreousness [7,16] and are all influenced by climatic conditions [17]. A number of agronomic components influence final productivity, including phenology (maturity) and plant architecture (plant height and lodging resistance). The majority of important agronomic traits, including yield, are controlled or influenced by multiple genes and are quantitatively inherited [18]. In addition, most are influenced by the environment and interactions between environmental and genetic (G×E) effects [19–23]. One of the most common methods currently used for dissection of quantitative agronomic and quality traits is the association mapping (AM) approach [24].

AM, originating in human genetics, was initially combined with linkage disequilibrium (LD) to identify the role of genes and linked markers for the determination of disease loci [25]. It is now widely used in plant and crop genetics. Some of the first studies based on LD mapping applied in plants were done in maize [26], rice [27] and oat [28]. AM has the main objective of determining, based on LD, correlations between genotypes and phenotypes in a panel of selected individuals [29]. It can support the development of new genetic markers for use in marker-assisted plant breeding [30]. It also facilitates the analysis of genetic variation underlying traits for further characterisation of the loci of interest [31].

Single nucleotide polymorphism (SNP) markers are commonly used in quantitative trait loci (QTL) mapping experiments [32,33] and genome-wide association studies (GWAS) for the detection of marker-trait associations (MTAs) in wheat [34–38]. DArTseq, a variant of the microarray-based DArT technology, has also been widely used in QTL mapping [39–41]. It reduces the complexity of the genome, using combinations of restriction enzymes [42] and next-generation sequencing. Several studies have assessed MTAs in durum wheat. The analyzed traits include grain yield, yield and yield components [6,37,43,44], heading date [6], and grain quality traits (thousand kernel weight, vitreousness, protein content, sedimentation index [17,45–47], yellow colour [48,49]).

In this study, three panels of elite durum wheat lines from CIMMYT were assessed in field trials conducted over multiple seasons and with differing water regimes. The AM approach was used to detect SNP and DArT markers associated with heterogeneous agronomic and quality trait data in order to test the approach as a tool for marker discovery within a live and ongoing breeding programme.

## 2. Material and Methods

### 2.1. Plant Material, Phenotyping and Genotyping

Panels of elite durum lines from CIMMYT wheat preliminary yield trials (PYT), comprising a total of 294 accessions (Supplementary Materials Table S1) were used for agronomic and quality assessment. PYT trials consisted of the best advanced breeding lines which were promoted to unreplicated trials, including one or two repeated checks. The trials were sown, assessed and analysed according to their specific statistical designs [50] and consisted of two blocks with different water treatments, one with full irrigation (FI) and the other with reduced irrigation (RI). In the FI treatment four to five irrigations were applied during the field season to maintain the optimal soil moisture conditions, whilst in the RI block a single irrigation was applied at planting, in order to ensure establishment. In both water treatments the irrigation was applied by gravity in furrows. The rainfall data ([https://www.meteoblue.com/en/weather/historyclimate/weatherarchive/ciudad-obreg%c3%b3n\\_mexico\\_4013704](https://www.meteoblue.com/en/weather/historyclimate/weatherarchive/ciudad-obreg%c3%b3n_mexico_4013704)) for the four

field seasons is included in Supplementary Materials Figure S1. The agronomic and quality assessment of the panels over seasons is summarised in Table 1.

**Table 1.** Agronomic and quality assessment of wheat field trials. The number of lines, year, location and water regime applied is shown.

Wheat Panel	No. of Assessed Lines	Field Season			
		2012	2013	2014	2015
1	98	YAQ-FI			
2	97		YAQ-FI	YAQ-FI YAQ-RI	
3	98		YAQ-FI	YAQ-FI YAQ-RI	YAQ-FI YAQ-RI

YAQ: Yaqui (Mexico); FI: Full irrigation; RI: Reduced irrigation.

Field experiments were conducted at CIMMYT's experimental station in the Yaqui Valley, Mexico (27.282848° N; 109.923878° W) over four field seasons (2012 to 2015 harvest years, inclusive). Wheat panels 2 and 3 were phenotypically assessed across years, while panel 1 was only grown in 2012. The experimental plots (1.6 × 3 m) were sown in November/December of each year and harvested in May of the following year. Data for yellow rust were assessed in semi-controlled conditions at CIMMYT's experimental station in Toluca (Mexico).

Plant material for genetic analysis was harvested for each line at the 4th leaf stage (growth stage 14 on the Zadoks scale [51]) and immediately frozen in dry-ice. Samples were stored at −80 °C until DNA extraction. Approximately 100 mg of frozen tissue was used for DNA isolation with a DNeasy Plant Mini Kit from Qiagen, following the manufacturer's protocol. DNA sample quality and concentration were assessed using electrophoresis on a 0.8% agarose gel and the restriction enzyme Tru1I (ThermoFisher) was used to check for the absence of nucleases in DNA prior to genotyping.

Samples were genotyped by Diversity Arrays Technology Pty Ltd. (Montana St, University of Canberra, Bruce ACT 2617, Australia) (DArT) using DartSeq™. A total of 35,509 polymorphic dominant DArT markers and 9142 biallelic SNP markers were generated. Both datasets were thinned by removing one marker from each pair with a correlation coefficient of >0.95. The final dataset consisted on 14,588 DArT markers (of which 8411 were mapped) and 5716 SNP markers (4142 mapped markers). DartSeq™ genotyping and mapping of the corresponding markers to the wheat reference genome sequence RefSeq v1 from the International Wheat Genome Sequencing Consortium (IWGSC, <http://www.wheatgenome.org/>) was performed by DArT (diversityarrays.com), as described by Sukumaran et al. [43]. The distribution of markers across the A and B subgenomes is given in Table 2.

**Table 2.** Molecular markers distribution across the wheat genome. The distribution of DArT (Diversity Arrays Technology, left) and single nucleotide polymorphism (SNP, right) markers across the durum wheat A and B subgenomes and the number of unmapped markers are shown.

Chr	DArT Markers				SNP Markers			
	A	B	Un	Total <sup>1</sup>	A	B	Un	Total <sup>1</sup>
1	377	866	37	1280	193	444	16	653
2	563	791	69	1423	320	375	19	714
3	496	818	33	1347	250	352	11	613
4	585	325	10	920	283	171	4	458
5	312	725	13	1050	162	376	2	540
6	449	690	21	1160	262	308	5	575
7	623	573	35	1231	293	287	9	589
<b>Total <sup>2</sup></b>	3405	4788	218	8411	1763	2313	66	4142
<b>Un</b>				6177				1574
<b>Total</b>				14,588				5716

Chr: chromosome; A: wheat A subgenome; B: wheat B subgenome; Un: unmapped; <sup>1</sup>: total markers by group; <sup>2</sup>: total markers by genome.

## 2.2. Phenotypic Data

Ten agronomic and quality traits were assessed for three durum wheat elite line panels: days to heading (days, DTH); plant height (cm, PH); lodging (%; LOD); yellow rust (%; YR); yellow colour (YC); sedimentation index (cm<sup>3</sup>, SDS); sedimentation volume (cm<sup>3</sup>, SV); grain protein content (%; GPC); thousand kernel weight (g, TKW); and grain yield (Kg/ha, GY). Agronomic traits (DTH, PH, LOD, YR, TKW and GY) were assessed under both water treatments (FI and RI), and quality traits (YC, SV, SDS and GPC) were only evaluated under FI conditions. Visual disease evaluation and phenology assessments were made in the field, while quality parameters were evaluated on grain samples post-harvest. DTH, PH and LOD and YR were visually assessed at the field trials in Yaqui, while YR was assessed at Toluca. To assess DTH, heading date was recorded as the time when 50% of the spikes have emerged from the flag leaf sheath (stage 59 in Zadoks scale [51]); PH was recorded by measuring the distance between the stem's base and the top of the spike (awns not included); LOD was assessed as the percentage of lodging plot; and YR was assessed as the percentage of leaves with rust pustules. YC was assessed by a rapid colorimetric method with a Minolta color meter following CEN/TS 15,465:2008 [52–54]; SDS was evaluated following UNE 34,903:2014 [55,56]; SV and GPC were assessed by Near-infrared spectroscopy (NIRs) [57]; TKW was measured by weighing 2 samples of 100 entire kernels randomly chosen previously dried at 70 °C for 48 h.

The correlation between the assessed traits was analysed using the 'cor' function in R [58–60]. Then, an analysis of variance (ANOVA) was undertaken, using the 'aov' function in R [61], to obtain the descriptive statistics for each trait.

Traits were analysed using a Q + K linear mixed-model [62,63] which follows the model equation:

$$y = X\beta + S\alpha + Qv + Z\mu + \varepsilon \quad (1)$$

where  $y$  is a vector of observed phenotypes;  $X$ ,  $S$  and  $Z$  are matrices related to  $\beta$ ,  $\alpha$  and  $\mu$ , respectively;  $\beta$  is a vector of fixed effects;  $\alpha$  is a vector of marker effects;  $Qv$  is a vector of population effect;  $\mu$  is a vector of polygenic effects (with covariance proportional to a kindship or relationship matrix); and  $\varepsilon$  is a vector of residuals.

These analyses were carried out using GenStat (14th Edition) to generate the best linear unbiased estimates (BLUEs) of variety performance in different ways: (i) across years and blocks; (ii) across years for each block (FI and RI); (iii) across a reduced dataset (years 2013 and 2014) and blocks; and (iv) across the reduced dataset for each block. The resulting datasets (available in Supplementary Material Table S2) were then used in different association mapping analyses.

## 2.3. Population Structure and Linkage Disequilibrium

Population structure was assessed using principal component analysis (PCA) based on the combined DArT and SNP genotyping datasets. Euclidean distances were calculated using the R package 'ggfortify' [64] and the PCA was visualised with 'ggplot2' [65].

The pattern of linkage disequilibrium (LD) was assessed between each pair of SNP markers on the same chromosome across the two constitutive genomes with the allele frequency correlation ( $r^2$ ) using the 'popgen' package in R [66]. A heatmap was obtained with the  $D'$  and  $r^2$  values for each chromosome and a scatterplot to determine LD decay (genetic distance in cM).

## 2.4. Association Mapping (AM)

The AM analyses were performed on the BLUEs obtained above using an additive model with 'rrBLUP' [67] and 'GWASpoly' [68] packages in R in different ways. Two marker-based kinship matrices (k-matrix), created from a subset of 14,588 DArT and 5716 SNP markers, respectively, were used for the adjustment based on relatedness of individuals (Supplementary Materials Tables S3 and S4). A minor allele frequency (maf) threshold of 0.05 was used. To establish a  $p$ -value detection threshold

for statistical significance of associations, the Bonferroni correction, which employs a threshold of  $\alpha/m$  to ensure the genome-wide type error I of 0.05, was applied with a total of 1000 permutations.

Associated DartSeq<sup>TM</sup> and SNP markers were blasted against the wheat reference assembly RefSeqv1 [69] with no indels or mismatches allowed, using an ad hoc Java program, to confirm their physical mapping location on the A or B genomes. The molecular markers were also mapped against the durum wheat genome (<https://www.interomics.eu/durum-wheat-genome>) to confirm their physical positions. In addition, to identify candidate genes, results were filtered, selecting the hits with best *e*-value for each molecular marker, and candidate genes were manually selected based on their annotations.

### 3. Results

#### 3.1. Phenotypic Assessment

Results from the ANOVA for all the traits across years and water treatments are shown in Table 3. The mean phenotypic values across years were calculated for each block and panel to evaluate the influence of water conditions on the assessed traits (Table 3). Days to heading during the field seasons assessed ranged from 63 to 94 days. In plots with lower water availability (RI block), the spike emergence from the flag leaf took place approximately 11 days earlier than in FI plots. Plant height ranged from 39 to 110 cm showing differences between water regimes, with a decrease of 25–30 cm under RI conditions. Likewise, and as result of the RI treatment, GY (ranging from 1.35 to 10.63 ton/ha) and TKW (from 29.6 to 63.2 g) also varied, being reduced by 4–5 tons/ha and 7–10 g, respectively, in the low water availability RI treatment. This strong RI treatment resulted in very low heritability values for DTH, PH and LOD.

Several significant phenotypic correlations were observed between the analysed traits (Figure 1 and Supplementary Materials Table S5). The most correlated traits were PH and GY ( $r = 0.90$ ,  $p\text{-value} = <2.2 \times 10^{-16}$ ), followed by DTH and GY ( $r = 0.87$ ,  $p\text{-value} = <2.2 \times 10^{-16}$ ), SDS and SV ( $r = 0.85$ ,  $p\text{-value} = <2.2 \times 10^{-16}$ ) and also DTH and PH ( $r = 0.82$ ,  $p\text{-value} = <2.2 \times 10^{-16}$ ). Other traits showed important positive correlations too, including YC and DTH ( $r = 0.69$ ,  $p\text{-value} = 2.82 \times 10^{-9}$ ), GY and TKW ( $r = 0.66$ ,  $p\text{-value} = <2.2 \times 10^{-16}$ ), PH and TKW ( $r = 0.62$ ,  $p\text{-value} = <2.2 \times 10^{-16}$ ), GY and YC ( $r = 0.53$ ,  $p\text{-value} = 0.039$ ) and DTH and TKW ( $r = 0.49$ ,  $p\text{-value} = <2.2 \times 10^{-16}$ ). Negative correlations were also observed for SDS and GPC ( $r = -0.38$ ,  $p\text{-value} = <2.2 \times 10^{-16}$ ), and for GPC and YC ( $r = -0.08$ ,  $p\text{-value} = <2.2 \times 10^{-16}$ ) (Figure 1).

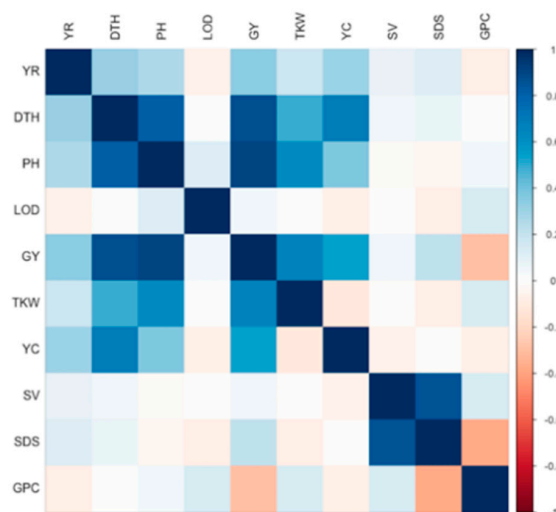


**Figure 1.** Phenotypic correlations. YR: yellow rust; DTH: days to heading; PH: plant height; GY: grain yield; TKW: thousand kernel weight; YC: yellow colour; SV: sedimentation volume; SDS: sedimentation index; and GPC: grain protein content.

**Table 3.** Summary of overall phenotypic data including analysis of variance (ANOVA) results and broad sense heritability ( $h^2$ ) for agronomic and quality traits.

	ANOVA										Mean Across Years				
	Min <sup>1</sup>	Mean <sup>2</sup>	Max <sup>3</sup>	Df	Sum Sq	Mean Sq	F Value	Pr (>F)	Significance	$h^2$					
<b>Panel</b>											1	2	2	3	3
<b>Water regimes</b>											FI	FI	RI	FI	RI
<b>DTH (days)</b>	63	79.38	94	1	1.8	1.768	0.24	0.626	***	0.14	87.55	83.73	72.54	81.95	70.51
<b>PH (cm)</b>	39	81.97	110	1	167.5	167.51	8.025	$6.59 \times 10^{-03}$	**	0.16	92.98	93.31	62.58	89.32	63.74
<b>GY (ton/ha)</b>	1.35	5.68	10.63	1	24.52	24.516	121.6	$4.16 \times 10^{-15}$	***	0.44	10	7	2.03	6	2.33
<b>TKW (g)</b>	29.6	44.69	63.2	1	38.6	38.65	2.064	$1.57 \times 10^{-01}$		0.41	49.25	47.58	37.29	47.06	40.22
<b>YR</b>	0	2.286	40	1	358.5	358.5	6.702	$1.25 \times 10^{-02}$	*	0.00	4.77	3.98	0	0	0
<b>LOD (%)</b>	0	2.142	90	1	0	0	-	-	-	0.01	0.1	0	0	9.25	0
<b>YC</b>	14.6	16.59	20	1	0.008	0.0085	0.02	$8.89 \times 10^{-01}$		0.59	17.21	17.09	-	16.35	-
<b>SV (ml)</b>	7	10.51	14.5	1	2.54	2.536	2.388	0.128		0.57	10.87	10.14	-	10.36	-
<b>SDS</b>	0.54	0.854	1.19	1	0.0927	0.09268	14.86	$3.25 \times 10^{-04}$	***	0.55	1	1	-	1	-
<b>GPC (%)</b>	10.4	12.33	14.9	1	5.965	5.965	16.41	$1.74 \times 10^{-04}$	***	0.31	11.67	12.38	-	12.12	-

DTH: days to heading; PH: plant height; LOD: lodging; GY: grain yield; TKW: thousand kernel weight; YR: yellow rust; LOD: lodging; YC: yellow color; SV: sedimentation volume; SDS: sedimentation index; GPC: grain protein content; FI: full irrigation block; RI: reduced irrigation block; <sup>1</sup>: minimum value across years and water regimes; <sup>2</sup>: mean across years and water regimes; <sup>3</sup>: maximum value across years and water regimes; Df: degrees of freedom; Sq: sum square; F value: measure of significance in the F-test; Pr (>F): *p*-value associated with the F statistic; Significance levels: 0 = '\*\*\*'; 0.001 = '\*\*'; 0.01 = '\*'; 0.1 = '.'; Df = degrees of freedom.

### 3.2. Population Structure and Linkage Disequilibrium

The PCA used a total of 14,588 DArT and 5716 SNP markers. The first and second principal components explained 3.91% of the genetic variation (Figure 2). No underlying genetic structure was detected within or between the panels assessed. LD was estimated using the mapped SNP markers dataset. LD decay was determined within 20–30 cM for all the chromosomes (Figure 3). Using the classification defined by Maccaferri et al. [70], the markers presented loose linkage (Class 2), showing a distance value between 21 to 50 cM.

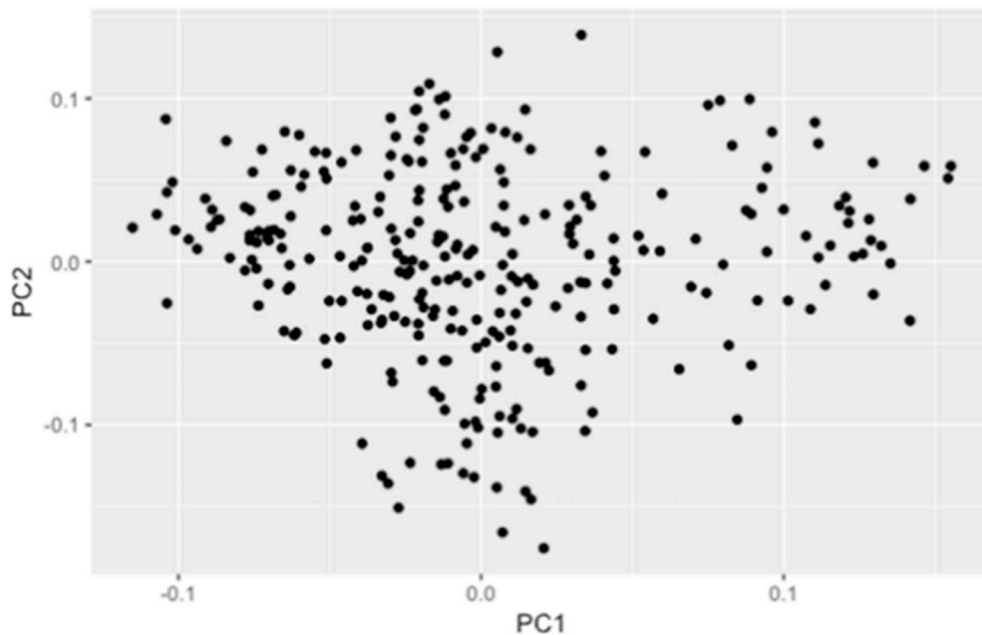


**Figure 2.** Principal components analysis (PCA) of the genotypic data.



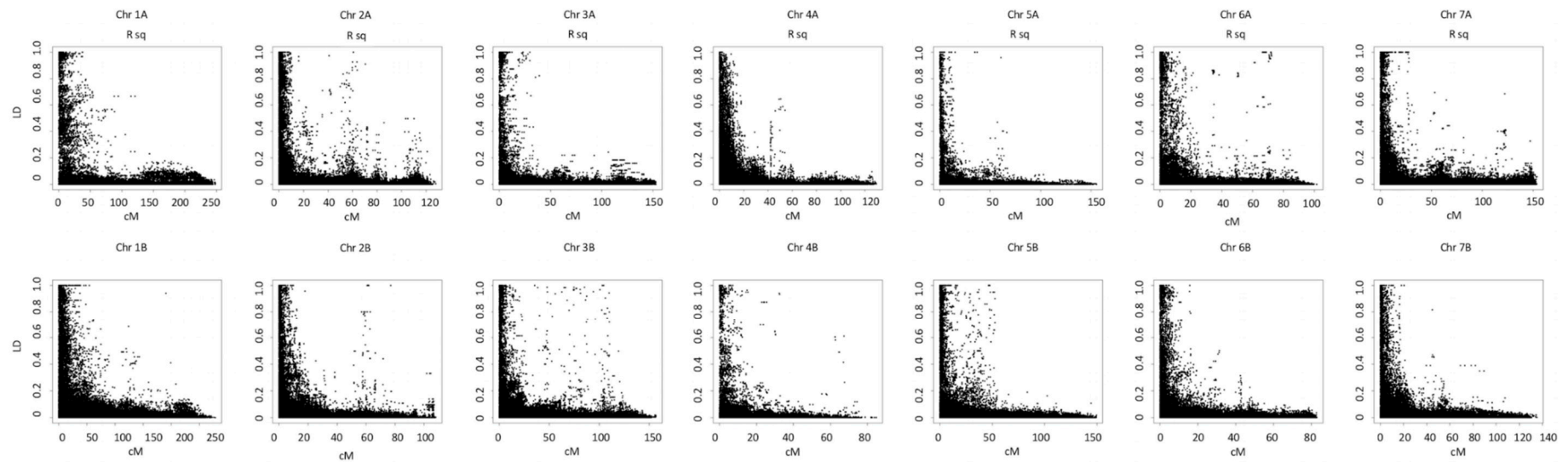


**Figure 3.** Linkage disequilibrium (LD) decay analysis using SNP data. Estimates  $r^2$  versus linkage distance on chromosome in centimorgan (cM) was represented. The LD decay was established between 20–30 cM.



### 3.3. AM Analysis

Thirty-seven significant marker-trait associations (MTAs) were detected for TKW and SV across all years and water treatments with most of the significant markers located on chromosome 2A (Table 4). Twenty DArT and seven SNP markers were found in association with TKW on chromosome 2A (with additive effects ranging from  $-3.41$  to  $3.46$ ). In addition, eight unmapped DArT and one SNP marker were also associated with TKW (additive effects ranged from  $-3.39$  to  $3.46$  g). Most of these MTAs showed a negative additive effect, reducing the final weight value (ranging from  $-2.84$  to  $-3.19$  g), and only two MTAs were found to increase TKW (values of  $2.97$  and  $3.09$  g). Finally, a single SNP associated with SV was located on chromosome 1B (showing a positive effect increasing the final value by  $1.26$  mL). The resulting Manhattan and QQ-plots from this AM analysis are included in Supplementary Materials Figures S2–S5.

The AM analyses on partitioned subsets of the data consistently detected the QTLs for TKW and SV. Nevertheless, the individual assessment of the water treatments significantly reduced the number of MTAs found, due in part to less available data for the RI block (Supplementary Material Table S6). The initial dataset of 294 durum wheat elite lines was reduced to 200 lines (assessed during the 2013 and 2014 seasons) to give a dataset balanced across assessment years. Using this reduced dataset for AM analysis, the results confirmed the QTLs previously found for the full dataset (Supplementary Materials Table S6). The analysis also detected an additional locus for SV on chromosome 4A, and a locus for YR on chromosome 1B (with additive effects of  $-0.84$  and  $2.79$ , respectively).

**Table 4.** Significant marker-trait associations found in durum wheat elite lines across years and water treatments.

Trait	Threshold	Marker	Chromosome	Pos (cM)	−log10 ( <i>p</i> -Value)	Marker Effect	Mapping in Pseudomolecule	Physical Pos (bp) <sup>1</sup>	Mapping in Durum	Physical Pos (bp) <sup>2</sup>
SV	5.09	SNP620	1B	139.21	5.5	1.26	1B	555,056,387	1B	547,593,323
TKW	5.71	DArT3154	2A	60.5	6.42	3.21	2A	533,610,520	2A	527,494,277
TKW	5.71	DArT3155	2A	60.5	6.11	−3.1	2A	174,036,184	2A	171,903,830
TKW	5.71	DArT3156	2A	60.5	7.28	−3.41	1B	134,638,820	1B	127,479,665
TKW	5.09	SNP1153	2A	68.47	5.38	−2.84	2A	582,636,674	2A	480,204,288
TKW	5.71	DArT3119	2A	68.91	6.77	−3.29	2A	536,825,718	2A	530,570,836
TKW	5.71	DArT3145	2A	69.27	7.1	3.43	2A	581,794,741	2A	550,694,987
TKW	5.71	DArT3146	2A	69.27	6.99	3.43	2A	566,208,089	2A	559,043,176
TKW	5.71	DArT3150	2A	69.42	7.23	3.4	2A	541,302,108	2A	535,046,952
TKW	5.71	DArT3162	2A	70.06	6.71	3.31	2A	535,235,854	2A	529,032,623
TKW	5.09	SNP1183	2A	70.31	6.45	−3.15	2A	541,200,911	2A	534,959,463
TKW	5.09	SNP1184	2A	70.31	6.79	−3.19	2A	541,391,854	2A	535,114,521
TKW	5.09	SNP1185	2A	70.31	5.45	−2.86	2A	532,153,681	2A	526,046,873
TKW	5.71	DArT3165	2A	70.31	7.17	3.46	2A	541,391,851	2A	534,959,463
TKW	5.71	DArT3169	2A	70.53	7	3.42	2B	477,405,138	2A	534,564,999
TKW	5.09	SNP1189	2A	70.84	6.46	−3.16	2A	542,687,204	2A	536,453,217
TKW	5.71	DArT3172	2A	70.96	5.91	3.13	2A	567,734,347	2A	557,502,938
TKW	5.71	DArT3174	2A	71.04	6.7	3.37	2A	566,457,122	2A	558,803,456
TKW	5.71	DArT3175	2A	71.14	6.13	3.2	2A	544,391,768	2A	538,104,252
TKW	5.71	DArT3176	2A	71.14	6.07	−3.17	2A	546,445,797	2A	540,140,599
TKW	5.71	DArT3180	2A	71.38	7.03	3.43	2A	567,736,123	2A	557,501,162
TKW	5.71	DArT3181	2A	71.38	6.2	3.2	2A	582,287,689	2A	551,184,512
TKW	5.71	DArT3182	2A	71.38	6.41	3.27	2A	569,404,524	2A	555,838,382
TKW	5.09	SNP1198	2A	71.64	6.39	3.09	2A	572,356,489	2A	552,887,972
TKW	5.09	SNP1199	2A	71.75	5.75	2.97	2A	567,787,911	2A	557,449,430
TKW	5.71	DArT3187	2A	71.94	7.07	3.35	2A	541,302,102	2A	535,046,946
TKW	5.71	DArT3198	2A	72.36	6.47	3.24	2A	535,235,860	2A	529,032,620
TKW	5.71	DArT3201	2A	72.56	6.19	3.12	2A	569,404,462	2A	555,838,444
TKW	5.71	DArT10906	-	-	6.16	−3.16	2A	566,964,200	2A	558,292,372
TKW	5.09	SNP8395	-	-	6.41	−2.85	2A	532,853,960	2A	526,751,856
TKW	5.71	DArT20759	-	-	7.23	3.4	2A	541,302,217	2A	535,047,061
TKW	5.71	DArT20961	-	-	7.17	3.46	2A	532,080,607	2A	525,972,283
TKW	5.71	DArT21317	-	-	6.06	3.18	2A	568,431,288	2A	556,806,491
TKW	5.71	DArT21609	-	-	7.04	−3.36	-	-	-	-
TKW	5.71	DArT21773	-	-	6.34	−3.17	-	-	-	-
TKW	5.71	DArT21834	-	-	6.35	−3.28	2A	546,445,800	2A	540,140,602
TKW	5.71	DArT22064	-	-	6.75	−3.39	-	-	2A	549,657,924

Pos (cM): position in chromosome in centimorgan; bp: base pairs; SV: sedimentation volume; TKW: thousand kernel weight; “-”: unmapped marker; <sup>1</sup>: physical position based on the wheat reference assembly RefSeqv1 [69]; <sup>2</sup>: physical position based on the durum wheat assembly [71].

### 3.4. Candidate Genes Analysis

The marker *SNP620*, located on chromosome 1B and detected in association with SV, was found included into a cluster of 12 genes encoding blue copper proteins (BCP), with homoeologs in the two durum wheat subgenomes (Figure 4, Table 5 and Supplementary Material Figure S6). In the hexaploid wheat genome, this set of genes form a cluster of homeolog triads [72] with a total of 31 genes (Supplementary Materials Table S7 and Figure S7). Additionally, another interesting gene (*TraesCS1B01G568400LC.1*) was found closer this marker, coding for the ubiquinone biosynthesis O-methyltransferase.

There were several markers located in chromosome 2A, in close proximity to some interesting genes. Markers *SNP1183*, *SNP1184* and *DArT3165* were found next to several genes encoding reductase-1 (Figure 4 and Table 5). In addition, the marker *SNP8395*, also located on the same chromosome, was found in proximity to the gene *TraesCS2A01G309700.1*, which encodes a type A response regulator 1 (Figure 4 and Table 5).

Significant MTAs from the partitioned analysis also allowed the identification of potentially interesting genes. On chromosome 1B, marker *DArT1744*, previously described by Mérida-García et al. [73] related to high molecular-weight glutenin subunits, was found in proximity to genes encoding isocitrate dehydrogenase kinase/phosphatase G and leucine-rich repeat receptor-like protein kinase family protein. These genes participate in the carbohydrate metabolism during the Krebs cycle and play a crucial role in plant development and stress responses, respectively [74,75]. On this chromosome, another marker (*SNP809*) was found in proximity to some interesting genes encoding sugar transporter proteins. Additionally, some markers located on chromosome 2A were found in proximity to Acyl-CoA N-acyltransferase genes (*SNP1206*, *SNP8395* and *DArT3180*) and chloroplastic zeaxanthin epoxidase (*SNP1189*) (Supplementary Materials Table S8).

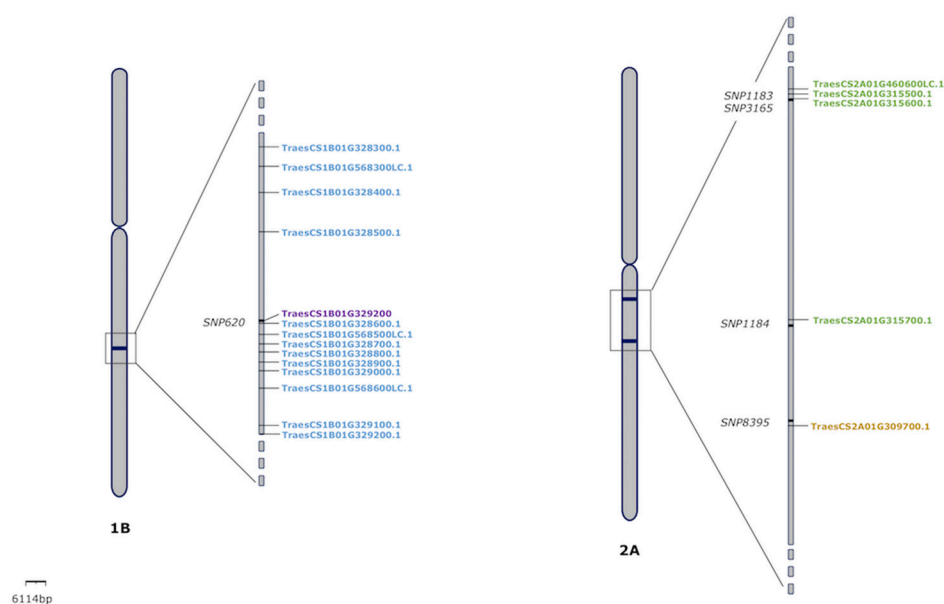


**Figure 4.** Location of candidate genes on chromosomes 1B and 2A. Markers are indicated with the symbol ‘-’; blue copper proteins are shown in blue colour; ubiquinone biosynthesis O-methyltransferase in purple colour; the regulator response gene in brown colour; and for reductase 1 genes in green colour.

**Table 5.** Candidate genes for markers with significant marker-traits associations. Genes located in proximity of markers found in association with TKW and SV across years and water treatments (within a  $\pm 50$  kb window). Values for physical position and distance are indicated in base pairs (bp). Chr: chromosome position. Blue copper proteins are shown in blue colour; ubiquinone biosynthesis *O*-methyltransferase in purple colour; the regulator response gene in brown colour; and for reductase 1 genes in green colour. Physical positions and gene annotations are based on the wheat reference assembly RefSeqv1 [69].

Marker	Identity	Transcript	Chr	Physical Position	Distance	Description
DArT3156	88.525	TraesCS1B01G193400LC.1	1B	134,604,832	−33,988	LINE-1 reverse transcriptase-like protein
		TraesCS1B01G193500LC.1	1B	134,605,786	−33,034	Retrotransposon protein. putative. unclassified
		TraesCS1B01G193600LC.1	1B	134,607,645	−31,175	Retrotransposon protein. putative. unclassified
		TraesCS1B01G193700LC.1	1B	134,621,105	−17,715	Retrotransposon protein. putative. unclassified
		TraesCS1B01G193800LC.1	1B	134,622,150	−16,670	Solute carrier organic anion transporter family member 2B1
		TraesCS1B01G193900LC.1	1B	134,622,613	−16,207	Tetratricopeptide repeat (TPR)-like superfamily protein
		TraesCS1B01G194000LC.1	1B	134,632,362	−6458	RNA-directed DNA polymerase (reverse transcriptase)-related family protein
		TraesCS1B01G194100LC.1	1B	134,633,505	−5315	LINE-1 reverse transcriptase like
		TraesCS1B01G194200LC.1	1B	134,639,730	910	Transposon Ty3-G Gag-Pol polypeptide
		TraesCS1B01G114900.1	1B	134,645,780	6960	F-box protein
		TraesCS1B01G194300LC.1	1B	134,648,368	9548	Sister chromatid cohesion protein PDS5 homolog B-B
		TraesCS1B01G194400LC.1	1B	134,649,000	10,180	BTB/POZ domain containing protein. expressed
DArT21834	100	TraesCS1B01G231000LC.1	1B	176,756,965	−3171	Retrotransposon protein. putative. LINE subclass
		TraesCS1B01G137700.1	1B	176,783,830	23,694	Phototropic-responsive NPH3 family protein
		TraesCS1B01G137700.2	1B	176,783,926	23,790	Phototropic-responsive NPH3 family protein
		TraesCS1B01G231100LC.1	1B	176,788,566	28,430	Disease resistance protein (TIR-NBS-LRR class) family
		TraesCS1B01G231200LC.1	1B	176,790,108	29,972	Transposon protein. putative. Mutator sub-class
		TraesCS1B01G231300LC.1	1B	176,790,698	30,562	Transposon protein. putative. mutator sub-class
		TraesCS1B01G231400LC.1	1B	176,791,607	31,471	Sterile alpha motif (SAM) domain-containing protein
		TraesCS1B01G137800.1	1B	176,793,792	33,656	GRF zinc finger family protein. expressed
		TraesCS1B01G231500LC.1	1B	176,803,822	43,686	Retrotransposon protein. putative. unclassified
SNP620	100	TraesCS1B01G568300LC.1	1B	555,010,255	−46,132	Blue copper protein
		TraesCS1B01G328400.1	1B	555,018,059	−38,328	Blue copper protein
		TraesCS1B01G328500.1	1B	555,029,816	−26,571	Blue copper protein
		TraesCS1B01G568400LC.1	1B	555,056,445	58	Ubiquinone biosynthesis <i>O</i> -methyltransferase
		TraesCS1B01G328600.1	1B	555,057,325	938	Blue copper protein
		TraesCS1B01G568500LC.1	1B	555,060,627	4240	Blue copper protein
		TraesCS1B01G328700.1	1B	555,063,537	7150	Blue copper protein
		TraesCS1B01G328800.1	1B	555,065,987	9600	Blue copper protein
		TraesCS1B01G328900.1	1B	555,068,889	12,502	Blue copper protein
		TraesCS1B01G329000.1	1B	555,071,391	15,004	Blue copper protein
		TraesCS1B01G568600LC.1	1B	555,076,734	20,347	Blue copper protein
		TraesCS1B01G329100.1	1B	555,088,083	31,696	Blue copper protein
		TraesCS1B01G329200.1	1B	555,090,695	34,308	Blue copper protein
		TraesCS1B01G568700LC.1	1B	555,095,491	39,104	purple acid phosphatase 23
		TraesCS1B01G568800LC.1	1B	555,096,179	39,792	Disease resistance protein (TIR-NBS-LRR class) family
		TraesCS1B01G568900LC.1	1B	555,097,247	40,860	Retrotransposon protein. putative. Ty3-gypsy subclass
		TraesCS1B01G569000LC.1	1B	555,098,272	41,885	Retrotransposon protein. putative. Ty3-gypsy subclass
		TraesCS1B01G569100LC.1	1B	555,101,471	45,084	50S ribosomal protein L2
		TraesCS1B01G569200LC.1	1B	555,103,053	46,666	LINE-1 reverse transcriptase like

Table 5. Cont.

Marker	Identity	Transcript	Chr	Physical Position	Distance	Description
DArT3155	93.939	TraesCS2A01G213400LC.1	2A	174,011,203	−24,981	Retrotransposon protein. putative. unclassified. expressed
		TraesCS2A01G213500LC.1	2A	174,024,497	−11,687	APOLLO
		TraesCS2A01G201000.1	2A	174,026,194	−9990	Cytochrome P450-like
		TraesCS2A01G213600LC.1	2A	174,034,039	−2145	Retrotransposon protein. putative. unclassified. expressed
		TraesCS2A01G213700LC.1	2A	174,039,127	2943	Cytochrome P450
SNP1153	98.551	TraesCS2A01G493000LC.1	2A	582,628,952	−7722	Retrotransposon protein. putative. Ty3-gypsy subclass
		TraesCS2A01G493100LC.1	2A	582,629,900	−6774	Retrovirus-related Pol polyprotein from transposon gypsy
		TraesCS2A01G493200LC.1	2A	582,630,406	−6268	Retrotransposon protein. putative. unclassified
		TraesCS2A01G493300LC.1	2A	582,630,979	−5695	Retrotransposon protein. putative. Ty3-gypsy subclass
		TraesCS2A01G344800.1	2A	582,634,003	−2671	RAN guanine nucleotide release factor
		TraesCS2A01G344900.1	2A	582,637,903	1229	Nucleosome assembly protein 1-like 1
DArT3119	95.652	TraesCS2A01G457700LC.1	2A	536,796,624	−29,094	Retrovirus-related Pol polyprotein LINE-1
DArT3146	100	TraesCS2A01G333200.1	2A	566,207,430	−659	Kinesin-like protein
		TraesCS2A01G333200.2	2A	566,209,291	1202	Kinesin-like protein
DArT3150	100	TraesCS2A01G460800LC.1	2A	541,301,644	−464	1-phosphatidylinositol-3-phosphate 5-kinase FAB1A
DArT3162	100	TraesCS2A01G457200LC.1	2A	535,217,367	−18,487	Acetylglutamate kinase-like protein
		TraesCS2A01G457300LC.1	2A	535,221,879	−13,975	LINE-1 reverse transcriptase like
		TraesCS2A01G457400LC.1	2A	535,222,237	−13,617	LINE-1 reverse transcriptase
		TraesCS2A01G311500.1	2A	535,240,748	4894	NAC domain protein.
SNP1183	100	TraesCS2A01G460600LC.1	2A	541,195,856	−5055	Reductase 1
		TraesCS2A01G315500.1	2A	541,197,465	−3446	Reductase 1
		TraesCS2A01G460700LC.1	2A	541,198,542	−2369	NADH dehydrogenase [ubiquinone] iron-sulfur protein 3. mitochondrial
		TraesCS2A01G315600.1	2A	541,200,447	−464	Reductase 1
SNP1184	100	TraesCS2A01G460900LC.1	2A	541,386,879	−4975	Serine-type endopeptidase inhibitor. putative
		TraesCS2A01G461000LC.1	2A	541,387,542	−4312	Aldose reductase
		TraesCS2A01G315700.1	2A	541,391,385	−469	Reductase 1
DArT3165	98.246	TraesCS2A01G460600LC.1	2A	541,195,856	−5055	Reductase 1
		TraesCS2A01G315500.1	2A	541,197,465	−3446	Reductase 1
		TraesCS2A01G460700LC.1	2A	541,198,542	−2369	NADH dehydrogenase [ubiquinone] iron-sulfur protein 3. mitochondrial
		TraesCS2A01G315600.1	2A	541,200,447	−464	Reductase 1
		TraesCS2A01G460900LC.1	2A	541,386,879	−4972	Serine-type endopeptidase inhibitor. putative
		TraesCS2A01G461000LC.1	2A	541,387,542	−4309	Aldose reductase
		TraesCS2A01G315700.1	2A	541,391,385	−466	Reductase 1
SNP1189	100	TraesCS2A01G316900.1	2A	542,642,276	−44,928	Phosphate carrier protein. mitochondrial
		TraesCS2A01G317000.1	2A	542,648,355	−38,849	Zeaxanthin epoxidase. chloroplastic
		TraesCS2A01G317000.2	2A	542,649,684	−37,520	Zeaxanthin epoxidase. chloroplastic
		TraesCS2A01G317000.3	2A	542,650,147	−37,057	Zeaxanthin epoxidase. chloroplastic
		TraesCS2A01G462000LC.1	2A	542,652,662	−34,542	AUGMIN subunit 6
		TraesCS2A01G317100.1	2A	542,654,847	−32,357	Mitochondrial carrier protein
		TraesCS2A01G317200.1	2A	542,658,154	−29,050	Phosphatase 2C family protein
		TraesCS2A01G317300.1	2A	542,686,655	−549	transmembrane protein

Table 5. Cont.

Marker	Identity	Transcript	Chr	Physical Position	Distance	Description
DArT3172	100	TraesCS2A01G333900.1	2A	567,725,771	−8576	RNA-dependent RNA polymerase
		TraesCS2A01G334000.1	2A	567,735,196	849	MLP protein
DArT3174	100	TraesCS2A01G333300.1	2A	566,454,172	−2950	F-box/RNI-like superfamily protein
		TraesCS2A01G481800LC.1	2A	566,461,411	4289	Transposon Ty3-G Gag-Pol polyprotein
		TraesCS2A01G481900LC.1	2A	566,462,897	5775	Craniofacial development protein 2
		TraesCS2A01G482000LC.1	2A	566,478,234	21,112	Retrotransposon protein. putative. unclassified
DArT3175	100	TraesCS2A01G319300.1	2A	544,359,272	−32,496	target of AVR-B operation1
		TraesCS2A01G464000LC.1	2A	544,395,881	4113	Retrotransposon protein. putative. unclassified
DArT3176	98.182	TraesCS2A01G464500LC.1	2A	546,477,078	31,281	Transposon Ty3-I Gag-Pol polyprotein
		TraesCS2A01G464600LC.1	2A	546,478,437	32,640	Transposon Ty3-I Gag-Pol polyprotein
		TraesCS2A01G464700LC.1	2A	546,479,163	33,366	Transposon Ty3-I Gag-Pol polyprotein
DArT3180	100	TraesCS2A01G333900.1	2A	567,725,771	−10,352	RNA-dependent RNA polymerase
		TraesCS2A01G334000.1	2A	567,735,196	−927	MLP protein
DArT3182	100	TraesCS2A01G483800LC.1	2A	569,357,751	−46,773	autoinhibited Ca(2+)-ATPase. isoform 4
		TraesCS2A01G335600.1	2A	569,363,189	−41,335	Zinc finger family protein
DArT3187	98.551	TraesCS2A01G460800LC.1	2A	541,301,644	−458	1-phosphatidylinositol-3-phosphate 5-kinase FAB1A
DArT3198	98.305	TraesCS2A01G457200LC.1	2A	535,217,367	−18,493	Acetylglutamate kinase-like protein
		TraesCS2A01G457300LC.1	2A	535,221,879	−13,981	LINE-1 reverse transcriptase like
		TraesCS2A01G457400LC.1	2A	535,222,237	−13,623	LINE-1 reverse transcriptase
		TraesCS2A01G311500.1	2A	535,240,748	4888	NAC domain protein.
DArT3201	100	TraesCS2A01G483800LC.1	2A	569,357,751	−46,711	autoinhibited Ca(2+)-ATPase. isoform 4
		TraesCS2A01G335600.1	2A	569,363,189	−41,273	Zinc finger family protein
DArT10906	98.551	TraesCS2A01G482500LC.1	2A	566,976,225	12,025	RNA-directed DNA polymerase (Reverse transcriptase)
		TraesCS2A01G333600.1	2A	566,986,482	22,282	Gibberellin-regulated protein 2
SNP8395	96.296	TraesCS2A01G309400.1	2A	532,849,120	−4840	Pentatricopeptide repeat-containing protein
		TraesCS2A01G309500.1	2A	532,854,936	976	Smr domain containing protein
		TraesCS2A01G309600.1	2A	532,859,077	5117	Acyl-CoA N-acyltransferase isoform 2
		TraesCS2A01G309600.2	2A	532,859,077	5117	Acyl-CoA N-acyltransferase isoform 2
		TraesCS2A01G309700.1	2A	532,865,797	11,837	Response regulator
DArT20759	97.619	TraesCS2A01G460800LC.1	2A	541,301,644	−573	1-phosphatidylinositol-3-phosphate 5-kinase FAB1A
DArT20961	100	TraesCS2A01G308900.1	2A	532,040,483	−40,124	Translocase of chloroplast
		TraesCS2A01G309000.1	2A	532,077,143	−3464	GTPase Der
		TraesCS2A01G309100.1	2A	532,085,578	4971	Protein NRT1/PTR FAMILY 1.1
		TraesCS2A01G309100.2	2A	532,085,909	5302	Protein NRT1/PTR FAMILY 1.1

#### 4. Discussion

The maintenance of crop production is a current and pressing need given growing populations and reduced availability of arable land [76]. There is an increasing need for breeding programs to improve yield potential and the adaptation of new varieties to different biotic and abiotic stresses [77]. Abiotic stresses, including drought and heat, are impacting productivity on the million hectares of wheat grown worldwide each year [78]. Detailed molecular and phenotypic characterization are valuable tools in the dissection of complex traits [79], and especially those that are influenced by water availability [14].

The improvement of key traits is essential for better end-use production quantity and quality in wheat [80]. In this study, we analysed a set of 10 agronomic and quality traits under full irrigation conditions (FI), with an additional six traits also assessed under low water availability (RI) in order to understand trait variation under contrasting water regimes in the CIMMYT durum wheat breeding programme. Irrigation conditions influenced some important yield and yield-related traits such as GY and TKW, as well as adaptive traits including DTH and PH (Table 3). The RI treatments had decreased final yields in line with previous observations [6,81]. Previous reports have also shown TKW to be reduced by high temperatures [17], most likely related to water availability. Groos et al. [82] assessed the genetic basis of grain yield and protein content in a segregating population of wheat RILs grown at six locations and also identified effects from G×E interactions involving protein content and yield. Our mean trait values corroborated this, with the highest values for GY recorded for FI blocks across panels (see Table 3). A similar trend was shown for DTH, PH and TKW, which decreased under low-water regimes.

Correlations between the assessed traits showed that GY was positively correlated with two different phenology traits (PH and DTH). This is in agreement with Maccaferri et al. [6], who showed important positive and negative correlations for GY and DTH, and also positive correlations for GY and PH in several environments with different water regimes. DTH and PH were also positively correlated (Supplementary Materials Table S5), with taller plants having a longer time period to the emergence of the tip of the spike stage.

Wheat TKW is an important yield component with a direct effect on grain yield [83,84]. In line with this, our results showed a significant and positive correlation between TKW and GY. However, the previously reported negative correlation between TKW and DTH [6] was not observed, potentially as result of temperatures and water availability from emergence to heading, and also from heading to harvest. Rharrabti et al. [17] previously highlighted a positive correlation between protein content and TKW, which is in agreement with the results obtained in the present study. They highlighted that warm temperatures during grain filling could negatively affect this correlation.

Significant associations between endosperm proteins (gliadin and glutenin subunits) and SV have been previously highlighted [85,86]. Here we found a positive correlation ( $r = 0.15$ ) between SV and GPC. This correlation is thought to be the result of grain protein content influencing the sedimentation volume value [87], which depends on the degree of protein hydration and oxidation [88]. Finally, for sedimentation index (SDS) analysis, we observed a negative correlation with protein content, in agreement with results presented by Rharrabti et al. [17,45]. This is also in agreement with Oelofse et al. [89] who highlighted the significant influence of protein content on the SDS sedimentation test [90–92].

The SNP and DArT markers used to analyze patterns of genetic structure (Figure 2) and LD (Figure 3) for the durum wheat lines revealed no detectable genetic structure and consistent patterns of LD across chromosomes (LD was estimated to extend ~20 cM). These results support the suitability of durum elite line sets currently in use in breeding programmes for the practical application of GWAs analysis. The rate of unmapped markers was lower for SNP than for DArT markers (27.5% vs. 42.0%, Table 2), indicating higher precision in genetically mapping SNP markers, probably as a result of co-dominance.



In the assessment of MTAs for quality and yield-related traits, different AM analyses were performed on subsets of the dataset. Several MTAs for SV and TKW were detected across years and water regimes, located on chromosomes 1B and 2A, respectively. All GWAS analyses corroborated the major QTLs previously detected, and reported two new QTLs, one for YR in chromosome 1B, and another for SV in chromosome 4A.

Associations on chromosome 1B were significant for wheat quality. There are known loci including Gli-B1/Glu-B3 on this chromosome, which are of great importance for some gliadin and glutenin subunits [93]. In fact, the candidate gene analysis reported the presence of a high molecular-weight glutenin subunit (HMW-GS) gene in the proximity of marker *DArT1744* (found to be significantly associated with SV and SDS), which was previously described by Mérida-García et al. [73] in association with specific weight. In line with this, Pogna et al. [93] highlighted the importance of Glu-B3 for determining protein quality with these endosperm proteins showing significant effects on SV, which also showed a high and positive correlation with SDS in our study (Figure 1 and Supplementary Materials Table S5). Likewise, Blanco et al. [86] reported three QTLs on chromosomes 1B, 6A and 7B (based on the analysis of 259 polymorphic markers) associated with SDS and SV in a recombinant inbred line population. In the present study, we found a SNP marker (*SNP620*) associated with SV, showing a positive additive effect of 1.26 (see Table 4) and also with SDS (marker effect of 0.11) (Supplementary Materials Table S6). This marker was previously placed on chromosome 1B, in the same location as MTAs for gluten index and sedimentation index [73]. Other previous studies, such as Reif et al. [94] and Fiedler et al. [95], also reported markers associated with SV on chromosome 1B, but with differing genetic positions. The additional locus for SV found on chromosome 4A (marker *DArT9459*) has not been previously reported.

Marker *SNP620*, significantly associated with SV, is located within a cluster of homoeolog gene triads coding for blue copper proteins (Table 5 and Supplementary Materials Figure S6). These proteins have been described containing a copper atom, and participate in redox processes [96], with a crucial role in the electron shuttle in plants [97]. In addition, Yao et al. [98] described the blue copper protein genes as the targets of miR408 in wheat, which is involved in the regulation of gene transcription required for heading time [99]. In our study *SNP620* was also found in proximity to a gene coding for an ubiquinone biosynthesis O-methyltransferase. Liu et al. [100] highlighted its crucial role as an electron transporter in the electron transport chain of the aerobic respiratory chain. This ubiquinone gene is involved in plant growth and development, is implied in chemical compounds biosynthesis and metabolism which are involved in plant responses to stress, and also participates in gene expression regulation and cell signal transduction [100].

On chromosome 1B we also found a significant MTA for yellow rust, in agreement with previous studies in durum and bread wheat, which placed different markers significantly associated with this trait, but in differing genetic positions [101–104]. The candidate gene analysis revealed the proximity of this marker (*SNP809*) to sugar transporter protein genes. Sugars are formed during the photosynthetic process and are essential for plant nutrition. The sucrose transport has been considered of great importance for plant productivity [105]. In line with this, the sucrose is involved in the gene expression regulation of the supposedly sugar-sensing pathway [106,107].

The majority of MTAs for TKW were located on chromosome 2A, showing both positive and negative effects. Previous studies have reported different markers in association with this quality trait, including a number mapped on chromosome 2A [38,108–110]. One of the markers found by Yao et al. [38] (SSR marker *gwm445* on chromosome 2A (68.2 cM), belongs to the same QTL found in this study for the marker *SNP1153* (chromosome 2A, 68.6 cM), and also found by Juliana et al. [111] in bread wheat lines from CIMMYT's first year-yield trials. Sukumaran et al. [43] analysed a durum wheat panel of 208 lines under yield potential, heat and drought stress conditions, and identified markers on chromosome 2A with a similar position to those detected in this study (4 markers at 70 cM and 6 markers at 69 cM) under heat stress conditions. They highlighted that several SNP markers were related to transmembranes or were uncharacterized proteins. We found several candidate genes for this

important TKW QTL (Table 5) among which the most striking feature is the presence of four reductase 1 genes (NADPH-dependent 6'-deoxychalcone synthase) and a type A response regulator 1 (Figure 4). These genes are both related with photosynthesis. Hu et al. [112] highlighted that NADPH plays a crucial role in biological processes in plants, such as the regulation of the production of reactive oxygen species (ROS) for the stress tolerance [113,114]. Additional GWAS analyses using reduced datasets revealed other interesting genes for this QTL (chromosome 2A, Supplementary Materials Table S8), encoding for the Acyl-CoA N-acyltransferase and the chloroplastic zeaxanthin epoxidase. The first gene has several functions in signaling and metabolic pathways [115]. The zeaxanthin epoxidase plays an important role in the xanthophyll cycle and abscisic acid (ABA) biosynthesis. The xanthophyll cycle has a main function in the dissipation of light energy excess and also increasing the photosynthetic system stability [116].

The proposed approach has successfully detected genetic markers with significant associations with TKW, SV, SDS and YR. These are of potential use in durum wheat breeding programs, and can be further interrogated to the candidate gene level using the RefSeqv1 bread wheat genome reference [69] and the durum wheat genome reference [71].

**Supplementary Materials:** The following are available online at <http://www.mdpi.com/2073-4395/10/1/144/s1>: Figure S1: Rainfall data for Ciudad Obregon (Mexico) for the growing seasons 2012–2015; Figure S2: Manhattan plots for durum wheat mapped DArT markers. DTH: days to heading; PH: plant height; GY: grain yield; TKW: thousand kernel weight; YC: yellow color; SV: sedimentation volume; SDS: sedimentation index; and GPC: grain protein content; Figure S3: Manhattan plots for durum wheat mapped SNP markers. DTH: days to heading; PH: plant height; GY: grain yield; TKW: thousand kernel weight; YC: yellow color; SV: sedimentation volume; SDS: sedimentation index; and GPC: grain protein content; Figure S4: Quantile quantile-plots from genome-wide association studies (GWAS) analysis for durum wheat DArT markers (mapped and unmapped). DTH: days to heading; PH: plant height; LOD: lodging; GY: grain yield; TKW: thousand kernel weight; YC: yellow color; SV: sedimentation volume; SDS: sedimentation index; and GPC: grain protein content; Figure S5: Quantile quantile-plots from GWAS analysis for durum wheat SNP markers (mapped and unmapped). DTH: days to heading; PH: plant height; LOD: lodging; GY: grain yield; TKW: thousand kernel weight; YC: yellow color; SV: sedimentation volume; SDS: sedimentation index; and GPC: grain protein content; Figure S6: Blue copper protein gene cluster on durum wheat chromosome 1B. High confidence genes are shown in green colour, low confidence genes are shown in yellow; Figure S7: Cluster tree of blue copper protein gene homoeologs in bread wheat (RefSeqv1 [69]). For chromosome 1A, high confidence (HC) and low confidence (LC) genes are shown in brown and orange colour, respectively; for chromosome 1B, HC and LC genes are shown in dark and light green colour, respectively; for chromosome 1D, HC and LC genes are shown in dark and light blue colour, respectively; Table S1: Durum wheat elite lines assessed; Table S2: Best Linear Unbiased Estimates (BLUEs) outputs for all assessed traits and the association mapping analyses performed in durum wheat: [i] across years and blocks; [ii] across years for each block (FI and RI); [iii] across years and blocks for a reduced dataset (years 2013 and 2014); and [iv] across the reduced dataset for each block. DTH: days to heading; GPC: grain protein content; GY: grain yield; PH: plant height; SDS: sedimentation index; SV: sedimentation volume; TKW: thousand kernel weight; and YC: yellow colour; YR: yellow rust; LOD: lodging; Table S3: Kinship matrix for durum wheat DArT markers; Table S4: Kinship matrix for durum wheat SNP markers; Table S5: Phenotypic correlations between the assessed traits in durum wheat and their corresponding p values. YR: yellow rust; DTH: days to heading; PH: plant height; LOD: lodging; GY: grain yield; TKW: thousand kernel weight; YC: yellow color; SV: sedimentation volume; SDS: sedimentation index; and GPC: grain protein content; Table S6: Marker-trait associations found for the association mapping analyses performed in durum wheat: [i] across years and blocks; [ii] across years for each block (FI and RI); [iii] across years and blocks for a reduced dataset (years 2013 and 2014); and [iv] across the reduced dataset for each block. SV: sedimentation volume; TKW: thousand kernel weight; SDS: sedimentation index; YR: yellow rust; “-”: unmapped marker; Table S7: Homoeolog triads for blue copper protein genes mapped in the wheat reference assembly RefSeqv1 [69]; Table S8: Candidate genes for GWAS analyses performed in durum wheat: [i] across years for each block (FI and RI); [ii] across years and blocks for a reduced dataset (years 2013 and 2014); and [iii] across the reduced dataset for each block. Molecular markers mapping positions are shown both in the durum wheat genome [71] and the wheat reference assembly RefSeqv1 [69]; Supplementary Material S1. R script used to perform the GWAS analysis; Supplementary Material S2. R script used to perform the LD analysis.

**Author Contributions:** P.H., I.S. and K.A. conceived the experiment. K.A. and I.S. selected the plant materials and agronomic traits. K.A. managed the field trials and contributed the phenotypic data. I.S., P.H., G.D., S.G., R.M.-G. and A.R.B. analysed the genotypic and phenotypic data. R.M.-G. isolated the DNA. R.M.-G., A.R.B. and P.H. carried out the AM analyses. R.M.-G., A.R.B. and P.H. drafted the manuscript. All authors have read and agreed to the published version of the manuscript.

**Funding:** This research was funded by project P12-AGR-0482 from Junta de Andalucía (Andalusian Regional Government), Spain (Co-funded by FEDER). ARB is supported by the UK Biotechnology and Biological Sciences Research Council (BBSRC) ‘Designing Future Wheat’ cross-institute strategic programme

(BB/P016855/1). PH is supported by the Spanish Ministry of Economy, Industry and Competitiveness (MINECO) project AGL2016-77149-C2-1-P.

**Conflicts of Interest:** The authors declare that the research was conducted in the absence of any commercial or financial relationships that could be construed as a potential conflict of interest.

## References

1. Curtis, B.C. Wheat in the world. In *Bread Wheat Improvement and Production*; Curtis, B.C., Rajaram, S., Gomez Macpherson, H., Eds.; Plant Production and Protection Series; Food and Agriculture Organization of the United Nations: Rome, Italy, 2002; Volume 30, pp. 1–17.
2. Ranieri, R. *Geography of Durum Wheat Crop*; Pastaria Open Fields: Collecchio, Italy, 2015.
3. Bozzini, A.; Fabriani, G.; Lintas, C. Origin, Distribution, and Production of Durum Wheat in the World. In *American Associate of Cereal Chemists International, Durum Wheat*, 2nd ed.; AACCI International Press: Saint Paul, MN, USA, 2012. [\[CrossRef\]](#)
4. Nachit, M.M. Durum wheat breeding for Mediterranean drylands of north Africa and west Asia. In *Durum Wheats: Challenges and Opportunities*; Rajaram, S., Saari, E.E., Hettel, G.P., Eds.; Wheat Special Report; CIMMYT: Ciudad Obregón, Mexico, 1992.
5. Singh, R.P.; Huerta-Espino, J.; Fuentes, G.; Duveiller, E.; Gilchrist, L.; Henry, M.; Nicol, M.J. Resistance to diseases. In *Durum Wheat Breeding: Current Approaches and Future Strategies*; Royo, C., Nachit, M.M., Fonzo, D., Araus, J.L., Er, W.H.P., Slafer, G.A., Eds.; Food Prod Press: Binghamton, NY, USA, 2005; pp. 291–315.
6. Maccaferri, M.; Sanguineti, M.C.; Demontis, A.; El-Ahmed, A.; Garcia del Moral, L.; Maalouf, F.; Nachit, M.; Nserallah, N.; Ouabbou, H.; Rhouma, S.; et al. Association mapping in durum wheat grown across a broad range of water regimes. *J. Exp. Bot.* **2011**, *62*, 409–438. [\[CrossRef\]](#)
7. Abdalla, O.; Dieseth, J.A.; Singh, R.P. Breeding durum wheat at CIMMYT. In *Durum Wheats: Challenges and Opportunities*; Rajaram, S., Saari, E.E., Hettel, G.P., Eds.; Wheat Special Report; CIMMYT: Ciudad Obregón, Mexico, 1992.
8. Wrigley, C.W. Wheat: An overview of the grain that provides our daily bread. In *Encyclopedia of Food Grains*; Colin, W., Wrigley, H.C., Koushik, S., Jonathan, F., Eds.; Elsevier: Oxford, UK, 2016; pp. 105–116. [\[CrossRef\]](#)
9. Tribioi, E.; Abad, A.; Michelena, A.; Lloveras, J.; Ollier, J.L.; Daniel, C. Environmental effects on the quality of two wheat genotypes: 1. quantitative and qualitative variation of storage proteins. *Eur. J. Agron.* **2000**, *13*, 47–64. [\[CrossRef\]](#)
10. Halford, N.G.; Curtis, T.Y.; Chen, Z.; Huang, J. Effects of abiotic stress and crop management on cereal grain composition: Implications for food quality and safety. *J. Exp. Bot.* **2015**, *66*, 1145–1156. [\[CrossRef\]](#)
11. Blumenthal, F.; Batey, I.L.; Wrigley, C.W.; Moss, H.J.; Mares, D.J.; Barlow, E.W.C. Interpretation of grain quality results from wheat variety trials with reference to high temperatures stress. *Aust. J. Agric. Res.* **1991**, *42*, 325–334. [\[CrossRef\]](#)
12. Campbell, C.A.; Davidson, H.R.; Winkleman, G.E. Effect of nitrogen, temperature, growth stage and duration of moisture stress on yield components and protein content of manitou spring wheat. *Can. J. Plant Sci.* **1981**, *61*, 549–563. [\[CrossRef\]](#)
13. Uhlen, A.K.; Hafskjold, R.; Kalhovd, A.H.; Sahlström, S.; Longva, Å.; Magnus, E.M. Effects of cultivar and temperature during grain filling on wheat protein content, composition, and dough mixing properties. *Cereal Chem.* **1998**, *75*, 460–465. [\[CrossRef\]](#)
14. Araus, J.L.; Slafer, G.A.; Royo, C.; Serret, M.D. Breeding for Yield Potential and Stress Adaptation in Cereals. *Crit. Rev. Plant Sci.* **2008**, *27*, 377–412. [\[CrossRef\]](#)
15. Curtis, T.; Halford, N.G. Food security: The challenge of increasing wheat yield and the importance of not compromising food safety. *Ann. Appl. Biol.* **2014**, *164*, 354–372. [\[CrossRef\]](#)
16. Steiger, D.K.; Elias, E.M.; Joppa, L.R.; Cantrell, R.G. Quality Evaluation of Lines Derived from Crosses of Langdon (*Triticum dicoccoides*) Substitution Lines to a Common Durum Wheat. In *Durum Wheats: Challenges and Opportunities*; Rajaram, S., Saari, E.E., Hettel, G.P., Eds.; Wheat Special Report; CIMMYT: Ciudad Obregón, Mexico, 1992.
17. Rharrabti, Y.; Villegas, D.; Royo, C.; Martos-Núñez, V.; Garcia del Moral, L.F. Durum wheat quality in Mediterranean environments II. Influence of climatic variables and relationships between quality parameters. *Field Crops Res.* **2003**, *80*, 133–140. [\[CrossRef\]](#)

18. Falconer, D.S.; Mackay, T.F.C. *Introduction to Quantitative Genetics*, 4th ed.; Pearson Education Limited: Harlow, UK, 1997; p. 464.
19. Borghi, B.; Corbellino, M.; Ciuffi, M.; La fiandra, D.; Destefanis, E.; Sgrulletta, D.; Boggini, G.; Di Fonzo, N. Effect of heat-shock during grain filling on grain quality of bread and durum wheats. *Aust. J. Agric. Res.* **1995**, *46*, 1365–1380. [\[CrossRef\]](#)
20. Garrido-Lestache, E.; Lopez-Bellido, R.J.; Lopez-Bellido, L. Durum wheat quality under Mediterranean conditions as affected by N rate, timing and splitting, N form and S fertilization. *Eur. J. Agron.* **2005**, *23*, 265–278. [\[CrossRef\]](#)
21. Holland, J.B. Genetic architecture of complex traits in plants. *Plant Biol.* **2007**, *10*, 156–161. [\[CrossRef\]](#)
22. Jackson, P.; Robertson, M.; Cooper, M.; Hammer, G. The role of physiological understanding in plant breeding: from a breeding perspective. *Field Crops Res.* **1996**, *49*, 11–39. [\[CrossRef\]](#)
23. Taghouti, M.; Gaboun, F.; Nsarellah, N.; Rhrib, R.; El-Haila, M.; Kamar, M.; Abbad-Andaloussi, F.; Udapa, S.M. Genotype x Environment interactin for quality traits in durum wheat cultivars adapted to different environments. *Afr. J. Biotechnol.* **2010**, *9*, 3054–3062.
24. Flint-Garcia, S.A.; Thuillet, A.C.; Yu, J.; Pressoir, G.; Romero, S.M.; Mitchell, S.E.; Doebley, J.; Kresovich, S.; Goodman, M.M.; Buckler, E.S. Maize association population: A high-resolution platform for quantitative trait locus dissection. *Plant J.* **2005**, *44*, 1054–1064. [\[CrossRef\]](#)
25. Bodmer, W.F. Human genetics: The molecular challenge. *BioEssays: News and Reviews in Molecular. Cell. Dev. Biol.* **1987**, *7*, 41–45. [\[CrossRef\]](#)
26. Bar-Hen, A.; Charcosset, A.; Bourgoin, M.; Guiard, J. Relationship between genetic markers and morphological traits in a Maize inbred lines collection. *Euphytica* **1995**, *84*, 145–154. [\[CrossRef\]](#)
27. Virk, P.S.; Ford-Lloyd, B.V.; Jackson, M.T.; Pooni, H.S.; Clemen, T.P. Predicting quantitative variation within rice germplasm using molecular markers. *Heredity* **1996**, *76*, 296–304. [\[CrossRef\]](#)
28. Beer, M.U.; Wood, P.J.; Weisz, J.; Fillion, N. Effect of cooking and storage on the amount and molecular weight of (1→3) (1→4)-D-glucan extracted from oat products by an in vitro digestion system. *Cereal Chem.* **1997**, *74*, 705–709. [\[CrossRef\]](#)
29. Zondervan, K.T.; Cardon, L.R. The complex interplay among factors that influence allelic association. *Nat. Rev. Genet.* **2004**, *5*, 89–100. [\[CrossRef\]](#)
30. Breseghello, F.; Sorrells, M.E. Association mapping of kernel size and milling quality in wheat (*Triticum aestivum* L.) cultivars. *Genetics* **2006**, *172*, 1165–1177. [\[CrossRef\]](#)
31. Maccaferri, M.; Sanguineti, M.C.; Mantovani, P.; Demontis, A.; Massi, A.; Ammar, K.; Kolmer, J.A.; Czembor, J.H.; Ezrati, S.; Tuberosa, R. Association mapping of leaf rust response in durum wheat. *Mol. Breed.* **2010**, *26*, 189–228. [\[CrossRef\]](#)
32. Marcotuli, I.; Gadaleta, A.; Mangini, G.; Signorile, A.M.; Zacheo, S.A.; Blanco, A.; Simeone, R.; Colasuonno, P. Development of a High-Density SNP-Based Linkage Map and Detection of QTL for beta-Glucans, Protein Content, Grain Yield per Spike and Heading Time in Durum Wheat. *Int. J. Mol. Sci.* **2017**, *18*, 1329. [\[CrossRef\]](#)
33. Liu, J.; Luo, W.; Qin, N.; Ding, P.; Zhang, H.; Yang, C.; Mu, Y.; Tang, H.; Liu, Y.; Li, W.; et al. A 55 K SNP array-based genetic map and its utilization in QTL mapping for productive tiller number in common wheat. *Theor. Appl. Genet.* **2018**, *131*, 2439–2450. [\[CrossRef\]](#)
34. Marcotuli, I.; Houston, K.; Schwerdt, J.G.; Waugh, R.; Fincher, G.B.; Burton, R.A.; Blanco, A.; Gadalena, A. Genetic Diversity and Genome Wide Association Study of beta-Glucan Content in Tetraploid Wheat Grains. *PLoS ONE* **2016**, *11*, e0152590. [\[CrossRef\]](#)
35. Poland, J.A.; Brown, P.J.; Sorrells, M.E.; Jannink, J.L. Development of high-density genetic maps for barley and wheat using a novel two-enzyme genotyping-by-sequencing approach. *PLoS ONE* **2012**, *7*, e32253. [\[CrossRef\]](#)
36. Somers, D.J.; Banks, T.; Depauw, R.; Fox, S.; Clarke, J.; Pozniak, C.; McCartney, C. Genome-wide linkage disequilibrium analysis in bread wheat and durum wheat. *Genome* **2007**, *50*, 557–567. [\[CrossRef\]](#)
37. Wang, S.X.; Zhu, Y.L.; Zhang, D.X.; Shao, H.; Liu, P.; Hu, J.B.; Zhang, H.; Zhang, H.P.; Chang, C.; Lu, J.; et al. Genome-wide association study for grain yield and related traits in elite wheat varieties and advanced lines using SNP markers. *PLoS ONE* **2017**, *12*, e0188662. [\[CrossRef\]](#)
38. Yao, J.; Wang, L.; Liu, L.; Zhao, C.; Zheng, Y. Association mapping of agronomic traits on chromosome 2A of wheat. *Genetica* **2009**, *137*, 67–75. [\[CrossRef\]](#)



39. Li, H.; Vikram, P.; Singh, R.P.; Kilian, A.; Carling, J.; Song, J.; Burgueno-Ferreira, J.A.; Bhavani, S.; Huerta-Espino, J.; Payne, T.; et al. A high density GBS map of bread wheat and its application for dissecting complex disease resistance traits. *BMC Genom.* **2015**, *16*, 216. [\[CrossRef\]](#)
40. Ren, R.; Ray, R.; Li, P.; Xu, J.; Zhang, M.; Liu, G.; Yao, X.; Kilian, A.; Yang, X. Construction of a high-density DArTseq SNP-based genetic map and identification of genomic regions with segregation distortion in a genetic population derived from a cross between feral and cultivated-type watermelon. *Mol. Genet. Genom.* **2015**, *290*, 1457–1470. [\[CrossRef\]](#) [\[PubMed\]](#)
41. Sanchez-Sevilla, J.F.; Horvath, A.; Botella, M.A.; Gaston, A.; Foltá, K.; Kilian, A.; Denoyes, B.; Amaya, I. Diversity Arrays Technology (DArT) Marker Platforms for Diversity Analysis and Linkage Mapping in a Complex Crop, the Octoploid Cultivated Strawberry (*Fragaria x ananassa*). *PLoS ONE* **2015**, *10*, e0144960. [\[CrossRef\]](#) [\[PubMed\]](#)
42. Kilian, A.; Huttner, E.; Wenzl, P.; Jaccoud, D.; Carling, J.; Caig, V.; Evers, M.; Heller-Uszynska, K.; Cayla, C.; Patarapuwadol, S.; et al. The fast and the cheap, SNP and DArT-based whole genome profiling for crop improvement. In *The Wake of the Double Helix: From the Green Revolution to the Gene Revolution, Proceedings of the International Congress Avenue Media, Bologna, Italy, 27–31 May 2005*; Tuberosa, R., Phillips, R.L., Gale, M., Eds.; Avenue Media: Bologna, Italy, 2005; pp. 443–461.
43. Sukumaran, S.; Reynolds, M.P.; Sansaloni, C. Genome-Wide Association Analyses Identify QTL Hotspots for Yield and Component Traits in Durum Wheat Grown under Yield Potential, Drought, and Heat Stress Environments. *Front. Plant Sci.* **2018**, *9*, 81. [\[CrossRef\]](#)
44. Turuspekov, Y.; Baibulatova, A.; Yermekbayev, K.; Tokhetova, L.; Chudinov, V.; Sereda, G.; Ganai, M.; Griffiths, S.; Abugalieva, S. GWAS for plant growth stages and yield components in spring wheat (*Triticum aestivum* L.) harvested in three regions of Kazakhstan. *BMC Plant Biol.* **2017**, *17* (Suppl. 1), 190. [\[CrossRef\]](#)
45. Johnson, M.; Kumar, A.; Oladzaad-Abbasabadi, A.; Salsman, E.; Aoun, M.; Manthey, F.A.; Elias, E.M. Association Mapping for 24 Traits Related to Protein Content, Gluten Strength, Color, Cooking, and Milling Quality Using Balanced and Unbalanced Data in Durum Wheat [*Triticum turgidum* L. var. durum (Desf)]. *Front. Genet.* **2019**, *10*. [\[CrossRef\]](#)
46. Mangini, G.; Gadaleta, A.; Colasuonno, P.; Marcotuli, I.; Signorile, A.M.; Simeone, R.; De Vita, P.; Mastrangelo, A.M.; Laido, G.; Pecchioni, N.; et al. Genetic dissection of the relationships between grain yield components by genome-wide association mapping in a collection of tetraploid wheats. *PLoS ONE* **2018**, *13*, e0190162. [\[CrossRef\]](#)
47. Mengistu, D.K.; Kidane, Y.G.; Catellani, M.; Frascaroli, E.; Fadda, C.; Pe, M.E.; Dell'Acua, M. High-density molecular characterization and association mapping in Ethiopian durum wheat landraces reveals high diversity and potential for wheat breeding. *Plant Biotechnol. J.* **2016**, *14*, 1800–1812. [\[CrossRef\]](#)
48. Pozniak, C.J.; Knox, R.E.; Clarke, F.R.; Clarke, J.M. Identification of QTL and association of a phytoene synthase gene with endosperm colour in durum wheat. *Theor. Appl. Genet.* **2007**, *114*, 525–537. [\[CrossRef\]](#)
49. Reimer, S.; Pozniak, C.J.; Clarke, F.R.; Clarke, J.M.; Somers, D.J.; Knox, R.E.; Singh, A.K. Association mapping of yellow pigment in an elite collection of durum wheat cultivars and breeding lines. *Genome* **2008**, *51*, 1016–1025. [\[CrossRef\]](#)
50. Van Ginkel, M.R.; Trethowan, R.; Cukadar, B. *A Guide to the CIMMYT Bread Wheat Program*; Wheat Special Report No 5; CIMMYT: Ciudad Obregón, Mexico, 1998.
51. Zadoks, J.C.; Chang, T.T.; Konzak, C.F. A decimal code for the growth stages of cereals. *Weed Res.* **1974**, *14*, 415–421. [\[CrossRef\]](#)
52. Henstchel, V.; Kranl, K.; Hollmann, J.; Lindhauer, M.G.; Bohm, V.; Bitsch, R. Spectrophotometric determination of yellow pigment content and evaluation of carotenoids by high-performance liquid chromatography in durum wheat grain. *J. Agric. Food Chem.* **2002**, *50*, 6663–6668.
53. Martinez, C.S.; Ribotta, P.D.; León, A.E.; Añón, M.C. Colour assessment on bread wheat and triticale fresh pasta. *Int. J. Food Prop.* **2010**, *15*. [\[CrossRef\]](#)
54. Beleggia, R.; Platani, C.; Nigro, F.; Papa, R. Yellow pigment determination for single kernels of durum wheat (*Triticum durum* Desf.). *Cereal Chem.* **2011**, *88*, 504–508. [\[CrossRef\]](#)
55. Axford, D.W.E.; McDermott, E.E.; Redman, D.G. Small-scale test for breadmaking quality of wheat. *Cereal Foods World* **1978**, *23*, 477–478.
56. Seabourn, B.W.; Xiao, Z.S.; Tilley, T.; Herald, T.J.; Park, S.H. A rapid, small-scale sedimentation method to predict bread-making quality of hard winter wheat. *Crop Sci.* **2012**, *52*, 1306–1315. [\[CrossRef\]](#)

57. Williams, P.C.; Norris, K. *Near Infrared Technology in the Agricultural and Food Industries*, 2nd ed.; American Association of Cereal Chemistry, Inc.: St Paul, MN, USA, 2001.
58. Becker, R.A.; Chambers, J.M.; Wilks, A.R. *The New S Language: A Programming Environment for Data Analysis and Graphics*; Wadsworth & Brooks/Cole: Pacific Grove, CA, USA, 1988.
59. Kendall, M.G. A new measure of rank correlation. *Biometrika* **1938**, *30*, 81–93. [\[CrossRef\]](#)
60. Kendall, M.G. The treatment of ties in rank problems. *Biometrika* **1945**, *33*, 239–251. [\[CrossRef\]](#)
61. Chambers, J.M.; Freeny, A.; Heiberger, R.M. Chapter 5: Analysis of Variance; Designed Experiment. In *Statistical Models in S*; Chambers, J.M., Hastie, T.J., Eds.; Wadsworth & Brooks/Cole: Pacific Grove, CA, USA, 1992; pp. 145–193.
62. Yu, J.; Pressoir, G.; Briggs, W.H.; Vroh Bi, I.; Yamasaki, M.; Doebley, J.F.; McMullen, M.D.; Gaut, B.S.; Nielsen, D.M.; Holland, J.B.; et al. A unified mixed-model method for association mapping that accounts for multiple levels of relatedness. *Nat. Genet.* **2006**, *38*, 203–208. [\[CrossRef\]](#)
63. Kang, H.M.; Zaitlen, N.A.; Wade, C.M.; Kirby, A.; Heckerman, D.; Daly, M.J.; Eskin, E. Efficient control of population structure in model organism association mapping. *Genetics* **2008**, *178*, 1709–1723. [\[CrossRef\]](#)
64. Horikoshi, M.; Tang, Y. ggfortify: Data Visualization Tools for Statistical Analysis Results. *R J.* **2016**, *8*, 474–489.
65. Wickham, H. *Ggplot2: Elegant Graphics for Data Analysis*; Springer: New York, NY, USA, 2009.
66. Marchini, J.L. Popgen: Statistical and Population Genetics. R Package Version 1.0-3. 2013. Available online: <http://CRAN.R-project.org/package=popgen/> (accessed on 14 January 2020).
67. Endelman, J.B. Ridge regression and other kernels for genomic selection with R package rrBLUP. *Plant Genome* **2011**, *4*, 250–255. [\[CrossRef\]](#)
68. Rosyara, U.R.; De Jong, W.S.; Douches, D.S.; Endelman, J.B. Software for Genome-Wide Association Studies in Autopolyploids and Its Application to Potato. *Plant Genome* **2016**, *9*. [\[CrossRef\]](#) [\[PubMed\]](#)
69. Appels, R.; Eversole, K.; Feuillet, C.; Keller, B.; Rogers, J.; Stein, N.; Pozniak, C.J.; Choulet, F.; Distelfeld, A.; Poland, J.; et al. Shifting the limits in wheat research and breeding using a fully annotated reference genome. *Science* **2018**, *361*, eaar7191.
70. Maccaferri, M.; Sanguineti, M.C.; Noli, E.; Tuberosa, R. Population structure and long-range linkage disequilibrium in a durum wheat elite collection. *Mol. Breed.* **2005**, *15*, 271–290. [\[CrossRef\]](#)
71. Maccaferri, M.; Harris, N.S.; Twardziok, S.O.; Pasam, R.K.; Gundlach, H.; Spannagl, M.; Ormanbekova, D.; Lux, T.; Prade, V.M.; Milner, S.G.; et al. Durum wheat genome highlights past domestication signatures and future improvement targets. *Nat. Genet.* **2019**, *51*, 885–895. [\[CrossRef\]](#)
72. Galvez, S.; Merida-Garcia, R.; Camino, C.; Borrill, P.; Abrouk, M.; Ramirez-Gonzalez, R.H.; Biyikliglu, S.; Amil-Ruiz, F.; Dorado, G.; Budak, H.; et al. Hotspots in the genomic architecture of field drought responses in wheat as breeding targets. *Funct. Integr. Genom.* **2019**. [\[CrossRef\]](#)
73. Mérida-García, R.; Guozheng, L.; He, S.; González-Dugo, V.; Dorado, G.; Gálvez, S.; Solís, I.; Zarco-Tejada, P.; Reif, J.C.; Hernández, P. Genetic dissection of agronomic and quality traits based on association mapping and genomic selection approaches in durum wheat grown in Southern Spain. *PLoS ONE* **2019**. [\[CrossRef\]](#)
74. Ikeda, T.; Laporte, D.C. Isocitrate Dehydrogenase Kinase/Phosphatase: AceK alleles that express kinase but not phosphatase activity. *J. Bacteriol.* **1991**, 1801–1806. [\[CrossRef\]](#)
75. Liu, P.L.; Du, L.; Huang, Y.; Gao, S.M.; Yu, M. Origin and diversification of leucine-rich repeat receptor-like protein kinase (LRR-RLK) genes in plants. *BMC Evol. Biol.* **2017**, *17*, 47. [\[CrossRef\]](#)
76. Cassman, K.G.; Dobermann, A.; Walters, D.T.; Yang, H. Meeting cereal demand while protecting natural resources and improving environmental quality. *Annu. Rev. Environ. Resour.* **2003**, *28*, 315–358. [\[CrossRef\]](#)
77. Araus, J.L.; Slafer, G.A.; Reynolds, M.P.; Royo, C. Plant Breeding and Drought in C3 Cereals: What Should We Breed For? *Ann. Bot.* **2002**, *89*, 925–940. [\[CrossRef\]](#) [\[PubMed\]](#)
78. Ortiz, R.; Sayre, K.D.; Govaerts, B.; Gupta, R.K.; Subbarao, G.V.; Ban, T.; Hodson, D.; Dixon, J.; Ortiz-Monasterio, I.; Reynolds, M. Climate change: Can wheat beat the heat? *Agric. Ecosyst. Environ.* **2008**, *126*, 46–58. [\[CrossRef\]](#)
79. Alonso-Blanco, C.; Aarts, M.G.; Bentsink, L.; Keurentjes, J.J.; Reymond, M.; Vreugdenhil, D.; Koornneef, M. What has natural variation taught us about plant development, physiology, and adaptation? *Plant Cell* **2009**, *21*, 1877–1896. [\[CrossRef\]](#) [\[PubMed\]](#)
80. Amaya, A.; Peña, R.J. Utilization and quality of durum wheat. In *Durum Wheats: Challenges and Opportunities*; Rajaram, S., Saari, E.E., Hettel, G.P., Eds.; Wheat Special Report; CIMMYT: Ciudad Obregón, Mexico, 1992.

81. Maccaferri, M.; Sanguineti, M.C.; Corneti, S.; Ortega, J.L.A.; Salem, M.B.; Bort, J.; DeAmbrogio, E.; García del Moral, L.F.; Demontis, A.; El-Ahmed, A.; et al. Quantitative trait loci for grain yield and adaptation of durum wheat (*Triticum durum* Desf.) across a wide range of water availability. *Genetics* **2008**, *178*, 489–511. [\[CrossRef\]](#)
82. Groos, C.; Robert, N.; Bervas, E.; Charmet, G. Genetic analysis of grain protein-content, grain yield and thousand-kernel weight in bread wheat. *Theor. Appl. Genet.* **2003**, *106*, 1032–1040. [\[CrossRef\]](#)
83. Sen, C.; Toms, B. Character association and component analysis in wheat (*Triticum aestivum* L.). *Crop. Res.* **2007**, *34*, 166–170.
84. Shamsi, K.; Petrosyan, M.; Noor-mohammadi, G.; Haghighparast, A.; Kobrace, S.; Rasekhi, B. Differential agronomic responses of bread wheat cultivars to drought stress in the west of Iran. *Afr. J. Biotechnol.* **2011**, *10*, 2708–2715.
85. Blanco, A.; de Giovanni, C.; Laddomada, B.; Sciancalepore, A.; Simeone, R.; Devos, K.M.; Gale, M.D. Quantitative trait loci influencing grain protein content in tetraploid wheats. *Plant Breed.* **1996**, *115*, 310–316. [\[CrossRef\]](#)
86. Blanco, A.; Bellomo, M.P.; Cenci, A.; De Giovanni, C.; D'Ovidio, R.; Iacono, E.; Laddomada, B.; Pagnotta, M.A.; Porceddu, E.; Sciancalepore, A.; et al. A genetic linkage map of durum wheat. *Theor. Appl. Genet.* **1998**, *97*, 721–728. [\[CrossRef\]](#)
87. Pasha, I.; Anjum, F.M.; Butt, M.S.; Sultan, J.I. Gluten quality prediction and correlation studies in spring wheats. *J. Food Qual.* **2007**, *30*, 438–449. [\[CrossRef\]](#)
88. Shewry, P.R.; Tatham, A.S. Wheat. In *The Royal Society of Chemistry*; Elsevier Science B.V.: Amsterdam, The Netherlands, 2000; pp. 335–339.
89. Oelofse, R.M.; Labuschagne, M.T.; van Deventer, C.S. Influencing factors of sodium dodecyl sulfate sedimentation in bread wheat. *J. Cereal Sci.* **2010**, *52*, 96–99. [\[CrossRef\]](#)
90. Cubadda, R.E.; Carcea, M.; Marconi, E.; Trivisonno, M.C. Influence of protein content on durum wheat gluten strength determined by the SDS sedimentation test and by other methods. *Cereal Foods World* **2007**, *52*, 273–277. [\[CrossRef\]](#)
91. Carter, B.P.; Morris, C.F.; Anderson, J.A. Optimizing the SDS sedimentation test for end-use quality selection in a soft white and club wheat-breeding program. *Cereal Chem.* **1999**, *76*, 907–911. [\[CrossRef\]](#)
92. De Villiers, O.T.; Laubscher, E.W. Use of the SDSS test to predict the protein content and bread volume of wheat cultivars. *S. Afr. J. Plant Soil* **1995**, *12*, 140–142. [\[CrossRef\]](#)
93. Pogna, N.E.; Autran, J.C.; Mellini, F.; Lafiandra, D.; Feillet, P. Chromosome 1B-encoded gliadins and glutenins subunits. *J. Cereal Sci.* **1990**, *11*, 15–34. [\[CrossRef\]](#)
94. Reif, J.C.; Gowda, M.; Maurer, H.P.; Longin, C.F.; Korzun, V.; Ebmeyer, E.; Bothe, R.; Pietsch, C.; Wurschum, T. Association mapping for quality traits in soft winter wheat. *Theor. Appl. Genet.* **2010**, *122*, 961–970. [\[CrossRef\]](#)
95. Fiedler, J.D.; Salsman, E.; Liu, Y.; Michalak de Jimenez, M.; Hegstad, J.B.; Chen, B.; Manthey, F.A.; Chao, S.; Xu, S.; Elias, E.M.; et al. Genome-Wide Association and Prediction of Grain and Semolina Quality Traits in Durum Wheat Breeding Populations. *Plant Genome* **2017**, *10*. [\[CrossRef\]](#)
96. Sykes, A.G. Plastocyanin and the Blue Copper Proteins. In *Long-Range Electron Transfer in Biology. Structure and Bonding*; Springer: Berlin/Heidelberg, Germany, 1990; pp. 175–224. [\[CrossRef\]](#)
97. Feng, H.; Zhang, Q.; Wang, Q.; Wang, X.; Liu, J.; Li, M.; Huang, L.; Kang, Z. Target of ta-miR408, a chemocyanin-like protein gene (TaCLP1), plays positive roles in wheat response to high-salinity, heavy cupric stress and stripe rust. *Plant Mol. Biol.* **2013**, *83*, 433–443. [\[CrossRef\]](#)
98. Yao, Z.J.; Lin, R.M.; Xu, S.C.; Li, Z.F.; Wan, A.M.; Ma, Z.Y. The molecular tagging of the yellow rust resistance gene Yr7 in wheat transferred from differential host Lee using microsatellite markers. *Sci. Agric. Sin.* **2006**, *39*, 1146–1152.
99. Zhao, X.Y.; Hong, P.; Wu, J.Y.; Chen, X.B.; Ye, X.G.; Pan, Y.Y.; Wang, J.; Zhang, X.S. The ta-miR408-Mediated Control of TaTOC1 Genes Transcription Is Required for the Regulation of Heading Time in Wheat. *Plant Physiol.* **2016**, *170*, 1578–1594. [\[CrossRef\]](#)
100. Liu, G.; Zhao, Y.; Gowda, M.; Longin, C.F.H.; Reif, J.C.; Mette, M.F. Predicting hybrid performances for quality traits through genomic-assisted approaches in central European wheat. *PLoS ONE* **2016**, *11*, e0158635. [\[CrossRef\]](#) [\[PubMed\]](#)



101. Maccaferri, M.; Zhang, J.; Bulli, P.; Abate, Z.; Chao, S.; Cantu, D.; Bossolini, E.; Chen, X.; Pumphrey, M.; Dubcovsky, J. A genome-wide association study of resistance to stripe rust (*Puccinia striiformis* f. sp. *tritici*) in a worldwide collection of hexaploid spring wheat (*Triticum aestivum* L.). *G3 Genes Genomes Genet.* **2015**, *5*, 449–465. [\[CrossRef\]](#)
102. Liu, W.; Maccaferri, M.; Ryneerson, S.; Letta, T.; Zegeye, H.; Tuberosa, R.; Chen, X.; Pumphrey, M. Novel Sources of Stripe Rust Resistance Identified by Genome-Wide Association Mapping in Ethiopian Durum Wheat (*Triticum turgidum* ssp. *durum*). *Front. Plant Sci.* **2017**, *8*, 774. [\[CrossRef\]](#) [\[PubMed\]](#)
103. Godoy, J.G.; Ryneerson, S.; Chen, X.; Pumphrey, M. Genome-Wide Association Mapping of Loci for Resistance to Stripe Rust in North American Elite Spring Wheat Germplasm. *Phytopathology* **2018**, *108*, 234–245. [\[CrossRef\]](#)
104. Liu, W.; Naruoka, Y.; Miller, K.; Garland-Campbell, K.A.; Carter, A.H. Characterizing and Validating Stripe Rust Resistance Loci in US Pacific Northwest Winter Wheat Accessions (*Triticum aestivum* L.) by Genome-wide Association and Linkage Mapping. *Plant Genome* **2018**, *11*. [\[CrossRef\]](#)
105. Lemoine, R. Sucrose transporters in plants: Update on function and structure. *Biochim. Biophys. Acta* **1999**, *1465*, 246–262. [\[CrossRef\]](#)
106. Koch, K.E. Carbohydrate-modulated gene expression in plants. *Annu. Rev. Plant Physiol. Plant Mole Biol.* **1996**, *47*, 509–540. [\[CrossRef\]](#)
107. Smekens, S.; Rook, F. Sugar sensing and sugar-mediated signal transduction in plants. *Plant Physiol* **1997**, *115*, 7–13. [\[CrossRef\]](#)
108. Sun, X.-Y.; Wu, K.; Zhao, Y.; Kong, F.-M.; Han, G.-Z.; Jiang, H.-M.; Huang, X.-J.; Li, R.-J.; Wang, H.-G.; Li, S.-S. QTL analysis of kernel shape and weight using recombinant inbred lines in wheat. *Euphytica* **2008**, *165*, 615–624. [\[CrossRef\]](#)
109. Patil, R.M.; Tamhankar, S.A.; Oak, M.D.; Raut, A.L.; Honrao, B.K.; Rao, V.S.; Misra, S.C. Mapping of QTL for agronomic traits and kernel characters in durum wheat (*Triticum durum* Desf.). *Euphytica* **2013**, *190*, 117–129. [\[CrossRef\]](#)
110. Cui, F.; Fan, X.; Chen, M.; Zhang, N.; Zhao, C.; Zhang, W.; Han, J.; Ji, J.; Zhao, X.; Yang, L.; et al. QTL detection for wheat kernel size and quality and the responses of these traits to low nitrogen stress. *Theor. Appl. Genet.* **2016**, *129*, 469–484. [\[CrossRef\]](#) [\[PubMed\]](#)
111. Juliana, P.; Poland, J.A.; Huerta-Espino, J.; Shrestha, S.; Crossa, J.; Crespo-Herrera, L.; Henrique Toledo, F.; Govidan, V.; Mondal, S.; Kumar, U.; et al. Improving grain yield, stress resilience and quality of bread wheat using large-scale genomics. *Nat. Genet.* **2019**. [\[CrossRef\]](#) [\[PubMed\]](#)
112. Hu, C.H.; Wei, X.Y.; Yuan, B.; Yao, L.B.; Ma, T.T.; Zhang, P.P.; Wang, X.; Wang, P.Q.; Liu, W.T.; Li, W.Q.; et al. Genome-Wide Identification and Functional Analysis of NADPH Oxidase Family Genes in Wheat During Development and Environmental Stress Responses. *Front. Plant Sci.* **2018**, *9*, 906. [\[CrossRef\]](#) [\[PubMed\]](#)
113. Kaya, H.; Nakajima, R.; Iwano, M.; Kanaoka, M.M.; Kimura, S.; Takeda, S.; Kawarazaki, T.; Senzaki, E.; Hamamura, Y.; Higashiyama, T.; et al. Ca<sup>2+</sup>-activated reactive oxygen species production by Arabidopsis RbohH and RbohJ is essential for proper pollen tube tip growth. *Plant Cell* **2014**, *26*, 1069–1080. [\[CrossRef\]](#)
114. Gupta, D.K.; Pena, L.B.; Romero-Puertas, M.C.; Hernández, A.; Inouhe, M.; Sandalio, L.M. NADPH oxidases differentially regulate ROS metabolism and nutrient uptake under cadmium toxicity. *Plant Cell Environ.* **2017**, *40*, 509–526. [\[CrossRef\]](#)
115. Fu, W.; Shen, Y.; Hao, J.; Wu, J.; Ke, L.; Wu, C.; Huang, K.; Luo, B.; Xu, M.; Cheng, X.; et al. Acyl-CoA N-acyltransferase influences fertility by regulating lipid metabolism and jasmonic acid biogenesis in cotton. *Sci. Rep.* **2015**, *5*, 11790. [\[CrossRef\]](#)
116. Sui, N.; Li, M.; Meng, Q.-W.; Tian, J.-C.; Zhao, S.-J. Photosynthetic Characteristics of a Super High Yield Cultivar of Winter Wheat During Late Growth Period. *Agric. Sci. China* **2010**, *9*, 346–354. [\[CrossRef\]](#)

